

# The Angular Momentum Distribution within Halos in Different Dark Matter Models

D.N.Chen, Y.P. Jing

Shanghai Astronomical Observatory, the Partner Group of MPI für Astrophysik, Nandan  
Road 80, Shanghai 200030, China  
dnchen@center.shao.ac.cn; ypjing@center.shao.ac.cn

## ABSTRACT

We study the angular momentum profile of dark matter halos for a statistical sample drawn from a set of high-resolution cosmological simulations of  $256^3$  particles. Two typical Cold Dark Matter (CDM) models have been analyzed, and the halos are selected to have at least  $3 \times 10^4$  particles in order to reliably measure the angular momentum profile. In contrast with the recent claims of Bullock et al., we find that the degree of misalignment of angular momentum within a halo is very high. About 50 percent of halos have more than 10 percent of halo mass in the mass of negative angular momentum  $j$ . After the mass of negative  $j$  is excluded, the cumulative mass function  $M(< j)$  follows approximately the universal function proposed by Bullock et al., though we still find a significant fraction of halos ( $\sim 50\%$ ) which exhibit systematic deviations from the universal function. Our results, however, are broadly in good agreement with a recent work of van den Bosch et al.. We also study the angular momentum profile of halos in a Warm Dark Matter (WDM) model and a Self-Interacting Dark Matter (SIDM) model. We find that the angular momentum profile of halos in the WDM is statistically indistinguishable from that in the CDM model, but the angular momentum of halos in the SIDM is reduced by the self-interaction of dark matter.

*Subject headings:* galaxies:formation-galaxies:structure-galaxies:spiral-cosmology:theory- dark matter

## 1. Introduction

The formation of galactic disks is one of the most significant unsolved problems in cosmology. In the popular hierarchical clustering framework (White & Reese 1978),

disks form in the potential wells of dark matter halos while the baryons cool and collapse dissipatively (Fall & Efstathiou 1980). Assuming that the angular momentum of the gas is conserved during the collapse and that the gas has the same spin  $\lambda$  parameter as the dark matter in a halo, one can derive a density profile of cooled gas under an additional assumption that either the density profile is assumed to be exponential as observed or the angular momentum of dark matter within a halo follows a distribution, say, given by a uniform sphere in solid body rotation (e.g. Fall & Efstathiou 1980, Blumenthal et al. 1986, Dalcanton, Spergel, & Summers 1997, Jimenez et al. 1997, Mo, Mao, & White 1998; van den Bosch 1998; Avila-Reese & Firmani 2000). While the theory is quite successful in explaining many observational data of spiral galaxies (e.g. Mo, Mao, & White 1998), it has encountered two potentially serious difficulties.

It has been known for many years that detailed numerical simulations of gas collapse in Cold Dark Matter (CDM) models (Navarro & Benz 1991; Navarro & White 1994; Steinmetz & Navarro 1999; Navarro & Steinmetz 2000) have consistently indicated that the infalling gas loses too much angular momentum due to the dynamical friction, and the resulting disks are accordingly too small to be compatible with the observations. This discrepancy is known as the “angular momentum catastrophe” in disk galaxy formation (Navarro, & Benz 1991). It is unknown if this is a failure of CDM models (Sommer-Larsen & Dolgov 2001) or this is due to the simplified treatments of complicated gas physics in the simulations, e.g. gas heating from supernova explosion (Weil et al. 1998; Sommer-Larsen, Gelato & Vedel 1999; Mo & Mao 2002).

The second difficulty emerged recently after Bullock et al. (2001; hereafter B2001) claimed, based on a high-resolution simulation of a low density flat CDM model (LCDM), that the dark matter halos have a universal angular momentum profile, i.e. the mass distribution of specific angular momentum  $j$  in a halo obeys a universal form,

$$M(< j) = \frac{M_v \mu j}{j_0 + j} \quad (1)$$

where  $M_v$  is the virial mass,  $j_0 = (\mu - 1)j_{\max}$ , and  $j_{\max}$  is the maximum specific angular momentum. The parameter  $\mu$  indicates the shape of the profile. Under the conventional assumption that the angular momentum of the gas is the same as that of the dark matter before gas collapse and is conserved in detail during the collapse, the distribution (1) implies that the formed disks contain too much low angular momentum mass to be compatible with the high-resolution observations of galactic disks (Bullock et al. 2001, van den Bosch 2001; van den Bosch et al. 2001).

In this work we will examine the validity of equation (1) using independent simulation data. A large set of cosmological N-body simulations of the Standard Cold Dark Matter

(SCDM) model and a LCDM model (Jing & Suto 1998) are employed. The simulations have a similar resolution to that of B2001, but the sample used in this work is significantly larger. The large sample enables us to study the angular momentum profile by selecting a sample of halos which are well resolved. The two cosmological models will help to answer if the angular momentum profile of halos depends on cosmological parameters. We will also analyze the individual halo simulations (Jing & Suto 2000) in a Warm Dark Matter (WDM) model (Schaeffer & Silk 1988, Colombi, Dodelson & Widrow 1996, Sommer-Larsen & Dolgov 2001, Jing 2001, Avila-Reese et al. 2001, Bode, Ostriker, & Turok 2001) and in a Self-Interaction Dark Matter (SIDM) model (Spergel & Steinhardt 2000, Burkert 2000, Davé et al. 2001, Yoshida et al. 2000) to study if the angular momentum profile of halos is different in different dark matter models. These alternative dark matter models have been recently proposed to solve possible problems facing CDM models at sub-galactic scales, i.e. central steep density profiles of halos and too numerous sub-halos (Moore et al. 1999, Klypin et al. 1999).

Several similar works had appeared when the present work was near completion. Knebe et al. (2001) and Bullock et al. (2001b) have studied the angular momentum profile of halos in warm dark matter models which are similar to (but not the same as) ours. van den Bosch et al. (2002) also examined whether equation (1) is a good prescription for the angular momentum profile of halos in an N-body/hydrodynamic simulation. Since the simulations used by these authors are quite distinct, in terms of simulation volumes and simulation techniques, from those used in this paper, our work interestingly complements to theirs. Wherever necessary, we will compare with their results in the following sections.

The outline of this paper is as follows. The cosmological models and the numerical simulations are described in the next section. The methods for measuring the angular momentum profile and the results for the cosmological simulations are presented in section 3. In section 4, we discuss the results for the WDM and SIDM models. The conclusions are given in section 5.

## 2. Models and numerical simulations

One set of cosmological simulations used in this paper is from Jing & Suto (1998). Three CDM models were studied by Jing & Suto (1998), but here we consider only the SCDM and LCDM models. The SCDM is the (ever) standard CDM model, and the LCDM is a currently popular flat low-density model with the density parameter  $\Omega_0 = 0.3$  and the cosmological constant  $\lambda_0 = 0.7$ . The shape parameter  $\Gamma = \Omega_0 h$  and the amplitude  $\sigma_8$  (the rms top-hat density fluctuation of radius  $8 h^{-1} \text{Mpc}$  at the present time) of the linear

density power spectrum are 0.5 and 0.62 for the SCDM, and 0.2 and 1 for the LCDM. The simulations were generated with a vectorized P<sup>3</sup>M code using 256<sup>3</sup> simulation particles. The simulation boxsize is 100  $h^{-1}$ Mpc (hereafter SCDM100 and LCDM100), and there are three realizations for each model. After the work of Jing & Suto (1998), another set of simulations has been generated for a boxsize 50  $h^{-1}$ Mpc in these CDM models (hereafter SCDM50 and LCDM50). Each model has two realizations. The resolutions of these simulations are similar to that used by B2001 (i.e. 256<sup>3</sup> particles for a simulation box of 75  $h^{-1}$ Mpc).

The dark matter halo candidates are identified with the friends-of-friends method (FOF). A linking length  $b$  equal to 10% of the mean particle separation is adopted. For each candidate halo, we compute the gravitational potential for each particle and find the spherical over-density around the particle which has the potential minimum. The boundary of the candidate halo is determined as the sphere within which the mean density is equal to the virialization density  $\rho_v$ . According to the fitting formula of Bryan & Norman (1998) for  $\rho_v$ ,  $\rho_v = 101\rho_{\text{crit}}$  for the LCDM model and  $\rho_v = 178\rho_{\text{crit}}$  for the SCDM model, where  $\rho_{\text{crit}}$  is the critical density. Some of the candidate halos may overlap partly, i.e. the separation between two halos is less than the sum of their virial radii. If two halos are overlapped, the less massive halo is thrown away. Only the halos with the particle number  $N_v$  within the virial radius more than  $3 \times 10^4$  are included in our analysis. There are 183,243,307,215 halos in LCDM100, LCDM50, SCDM100 and SCDM50 respectively. For a comparison, B2001 used  $\sim 200$  halos with  $N_v \geq 6 \times 10^3$  and  $\sim 600$  halos with  $N_v \geq 10^3$ .

Since the accuracy of the angular momentum measurement critically depends on the mass resolution (i.e. the number of particles in a halo, cf. eq.4), and the angular momentum of a halo depends only weakly on its physical mass (as many previous studies of the spin parameter have shown), we combine the halos in LCDM100 and LCDM50, and form two samples according to the number of particles in halos. The first sample, called LCDM-CM, contains 10 halos with more than  $10^5$  particles, and the second one, called LCDM-C, contains all the halos (426) with more than  $3 \times 10^4$  particles. Similarly, two halo samples, called SCDM-CM and SCDM-C, are formed in the SCDM model, and they contain 27 and 522 halos respectively. A summary of the halo samples are given in Table 2.

In order to study whether the angular momentum of halos depends on the physical properties of dark matter, we use the sample of Jing (2001) for our analysis. Jing(2001) used the multi-mass particle code of Jing & Suto (2000) to re-simulate 15 halos in a WDM model. The WDM model has the same model parameters as the LCDM, except that the linear power spectrum is a WDM type with the free streaming scale  $R_f = 0.112 h^{-1}$ Mpc (corresponding to a particle mass 700eV; see Bardeen et al. 1986). The halos have mass  $5 \times 10^{12} h^{-1} M_\odot$ ,  $6 \times 10^{11} h^{-1} M_\odot$ , and  $7 \times 10^{10} h^{-1} M_\odot$  with five halos at each mass. About

$7 \times 10^5$  particles are used to simulate the halos with  $3 \times 10^5$  particles ended up within the virial radius. For an accurate comparison with the LCDM model, Jing (2001) also simulated 15 halos in the LCDM. The difference between the 15 LCDM halos and the 15 WDM halos is only the linear power spectrum, so each pair of the LCDM and WDM halos can be compared precisely to show the dependence on the input linear power spectrum. For details about the simulations, we refer readers to Jing (2001). We call the LCDM halos as LCDM-H halos, in order to distinguish them with those from the cosmological simulations.

The Self-Interaction Dark Matter (SIDM) model is the same as the LCDM, except that the dark matter may be self-interacting. First, five halos of mass  $5 \times 10^{12} h^{-1} M_\odot$  are selected from our LCDM simulation (Jing & Suto 1998), and are re-simulated with the multi-mass particle code. The halos have  $\sim 3 \times 10^5$  particles within the virial radius. The self-interactions are implemented in the code following Burkert (2000) and Davé et al. (2000). The parameter for the self-interaction is the cross section per unit of mass  $\sigma$ . We adopt  $\sigma = 0, 0.1, 1.0$ , and  $10 \text{ cm}^2/\text{g}$  for our simulation, and have the 5 halos simulated at each  $\sigma$ .

### 3. Results of cosmological simulations

A first step towards measuring the distribution of specific angular momentum within a halo is to measure its global angular momentum. The angular momentum of a halo of  $N$  particles is defined by

$$\mathbf{J} = \sum_i m_i \mathbf{r}_i \times \mathbf{v}_i \quad (2)$$

where  $\mathbf{r}_i$  and  $\mathbf{v}_i$  are the position and velocity of the  $i$ -th particle with respect to the halo center of mass. Following Mo et al. (1998; see also B2001), we measure the spin parameter  $\lambda$  according to the following formula

$$\lambda = \frac{J}{\sqrt{2} M_v V_c r_v} \quad (3)$$

where  $V_c$  is the circular velocity at the virial radius  $r_v$ .

The aim of the paper is to study how the angular momentum is distributed in a halo. Following B2001, we first determine the global angular momentum  $\mathbf{J}$  for each halo, and define the  $z$ -axis as pointing to the direction of  $\mathbf{J}$ . We then compute the distribution function of the mass  $M(< j)$  which has the specific angular momentum less than  $j$  along the  $z$ -axis. In order to measure the distribution function, we divide the spherical volume of each halo into 10 radial shells, each containing the same number of particles. Every radial shell is further divided into 6 azimuthal zones of equal solid angle between  $\cos \theta = -1$  and

1. The two zones with the same  $r$  and  $|\cos\theta|$  which are above and below the equatorial plane are assigned to one “cell”, and thus every halo is effectively divided into 30 cells each of which contains approximately the same number of particles.

The specific angular momentum  $j$  of a cell measures the bulk rotation (motion in the x-y plane) of the particles in the cell. A spin parameter  $\lambda \approx 0.04$  means that the bulk velocity is only a few percent of the random motion velocity of the particles. Thus, the discreteness of the particles would be the main source for the measurement error of  $j$  when the number of particles in the cell is not much more than  $10^3$ . For a halo of the circular velocity  $v_c(r)$  at the radius  $r$ , the error of  $j$  can be estimated by

$$\sigma_j = \frac{rv_c(r)}{\sqrt{N_c}} \quad (4)$$

where  $N_c$  is the particle number in the cell, and  $r$  is the mean distance of the cell from the halo center. This is likely an upper limit on the scatter, because the motion of particles is not completely random.

In Figure 1 and Figure 2, we show several examples of the angular momentum distribution functions in the two cosmological models. Each halo has more than  $10^5$  particles, so the signal-to-noise of the measurement is high. In the right panels, the cosine of the angle  $\theta$  between the angular momentum vector  $\mathbf{j}$  of a cell and the z-axis is presented. Among all the 426 LCDM halos, there are 68 halos (in the top-right panels) with all cells having  $\cos\theta > 0$ , so the angular momentum of the different cells aligns very well within these halos. This number is 108 out of 522 in the SCDM model. Also in 9 halos of LCDM model and 12 halos of SCDM model, (the third halos from the top), more than 50 % of the cells have  $\cos\theta < 0$ , i.e. the matter within these halos aligns very poorly. But in most of the halos, (i.e. 253 out of 426 halos in LCDM model and 319 out of 522 halos in SCDM model) about 10 to 20 percent of the cells have the negative angular momentum as the second halos from the top have shown. The fraction of the mass which has negative  $j$  is significantly higher than B2001 found. In their paper, B2001 claimed that “about 5% of halos have a significant amount of their total mass ( $\geq 10\%$ ) contained in negative  $j$  cells”. We note our results are in good agreement with a recent work of van den Bosch et al. (2002) who found a similar discrepancy with B2001, though their analysis is for halos of galactic mass and at redshift  $z = 3$ . The percentage of the matter having negative  $j$  will be discussed in more detail below. Since the fraction of negative  $j$  cells is non-negligible, the universal function (1) certainly fails for describing most of our halos, for the fitting formula assumes that the mass of anti-aligned  $j$  is negligible. Following B2001, we exclude all cells of negative  $j$  and compare the  $j$  distribution function with equation (1). In this case, we replace the virial mass  $M_v$  in the equation with the total mass of positive  $j$  cells  $M(j > 0)$ .

A comparison of our simulation result with the modified formula is presented in the left panels of the figures. Considering that the measurement of  $j$  in every cell has an error, when the cumulative mass  $M(< j)$  is considered, the error for the upper limit  $j$  might be underestimated if Eq.(4) is used. Conservatively, the error bars for the upper limit  $j$  in the figures are calculated by  $\sigma_{<j}^2 = \sum_{j_1 \leq j} \sigma_{j_1}^2$ . From the figure, it can be easily seen that the simulation data can be reasonably ( $\sim 50\%$ ) described by equation(1), but not perfectly. As the figures show, a significant fraction of halos has a higher fraction of low  $j$  mass than the fitting formula. Because the observational data of disk galaxies seem to indicate less low  $j$  mass than the function (1) (B2001, van den Bosch et al. 2001, van den Bosch 2001), our results imply that the discrepancy between the CDM models and the observations could be more serious unless some (unclear) physical mechanisms are in play to modify the  $j$  distribution of the gas which forms the discs (e.g. van den Bosch et al. 2002; Maller & Dekel 2002). Only a very small fraction (15 halos for LCDM model and 18 halos for SCDM model) of halos (e.g. the bottom examples in the figures) have less low  $j$  mass than the formula (1). These halos may be in a better agreement with the observational data of disk galaxies, but considering that the disk galaxies are common, it is unlikely that such halos are numerous enough to explain the observations.

In order to quantify how much mass in halos is contained in negative  $j$  cells, we present in Figure 3 the percentage of the halos which have a fraction of mass  $M(j < 0)/M_v$  in negative  $j$  cells. The upper panel shows for LCDM-H halos which have more than  $3 \times 10^5$  particles. Among the 15 halos, 12 halos have negative  $j$  cells and 4 halos have  $M(j < 0)/M_v$  higher than 10%. In the middle panel, we show the results for LCDM-C (the solid line) and LCDM-CM (the dotted line) samples. From the figure, it can be easily read that about 40% of LCDM-C halos and 55% of LCDM-CM halos have  $M(j < 0)/M_v > 0.1$ . Similarly, the percentage of the halos with  $M(j < 0)/M_v > 0.1$  is 50% in the SCDM-C and 60% in the SCDM-CM sample. We have further used the Kolmogorov-Smirnov test to make sure if there is any significant difference in the misalignment distribution between the different (sub)-samples. The test results, listed in Table 1, show that the distribution functions of the three subsamples in the LCDM model are consistent with being drawn from the same parent distribution. The distributions of the two subsamples in the SCDM model are also consistent. Therefore, the misalignment could not be a result from the discreteness effect in the simulations. Only significant difference has been found between SCDM-C and LCDM-C, since the both samples are large and there is significantly more misalignments of  $j$  in the SCDM-C.

The misalignments of  $j$  could be caused by the substructures in the halos. Since there is a higher amount of substructures in the SCDM than in the LCDM model (e.g. Jing et al. 1995), we can easily explain why the SCDM-C halo contain a higher fraction of

negative  $j$  mass than the LCDM-C halos. Following Jing (2000; hereafter J2000), we use the clumpiness of the density profile as an indicator for the substructures in halos. The clumpiness is quantified by the maximum relative deviation  $\text{dvi}_{\text{max}}$  of the simulation density profile  $\rho(r_i)$  from the fitting  $\rho_{\text{NFW}}(r_i)$  of the Navarro-Frenk-White (1996) form:

$$\text{dvi}_{\text{max}} = \max\left\{\left|\frac{\rho(r_i) - \rho_{\text{NFW}}(r_i)}{\rho_{\text{NFW}}(r_i)}\right|\right\} \quad (5)$$

where  $i$  runs over all radial bins of the density profile. Figure 4 plots the fraction of negative  $j$  mass in halos as a function of the substructure indicator  $\text{dvi}_{\text{max}}$ . Since most of the halos (401 out of 426 LCDM halos and 501 out of 522 SCDM halos) have  $\text{dvi}_{\text{max}} \leq 0.6$ , from the figure we find that the misalignment of  $j$  is nearly independent of the substructures. The peaks at  $\text{dvi}_{\text{max}} = 1.05$  in the LCDM model and at  $\text{dvi}_{\text{max}} = 0.75$  in the SCDM model may be contributed by statistical fluctuations, for there is only one halo in the LCDM peak and 7 halos in the SCDM peak.

We have also examined where the misalignment of  $j$  happens in halos. Figure 5 shows the percentage of negative  $j$  cells at different radius  $r$ . The results indicate that either at small or at large radii, there are more mass with negative  $j$  than at the median radius. The result can be easily understood, since the global angular momentum of a halo is mainly determined by the mass at the median radius, and the mass at the median radius will naturally align better with  $\mathbf{J}$ . This however indicates that the twisting of the angular momentum vectors occur everywhere inside halos.

It may also be interesting to study the distribution of the shape parameter  $\mu$  in the function  $M(< j)$  (Eq.1), and compare our results with B2001. We should emphasize again that only positive  $j$  cells are included in the fitting to our simulation results. In the function, we have replaced  $M_v$  in B2001 with  $M(j > 0)$ . The  $\mu - 1$  parameter follows a log-normal distribution (Figures 6 and 7) as what Bullock et al.(2001) found. The mean values  $\bar{\mu}$  and the scatter  $\sigma_{\ln(\mu-1)}$  are given in Figure 8 for LCDM and SCDM. From these two parameters, we can conclude that the distribution of  $\mu$  does not depend on the spin parameter  $\lambda$ . In the SCDM model  $\bar{\mu} = 1.27$  and  $\sigma_{\ln(\mu-1)} = 0.41$ , and in the LCDM model  $\bar{\mu} = 1.22$  and  $\sigma_{\ln(\mu-1)} = 0.41$ . We note that there is a tendency of the increase of  $\mu - 1$  with the spin parameter  $\lambda$  in B2001, which has not been confirmed by our analysis.

#### 4. Alternative dark matter models

As already pointed out in the previous section, the CDM models have the difficulty to explain the observational data of disk galaxies under the conventional assumption that the



angular momentum distribution of gas follows that of dark matter. While the assumption of gas tracing dark matter may well be wrong when realistic but complicated physical processes of galaxy formation are taken into account, we study here the angular momentum distribution in the Warm Dark Matter (WDM) model and in the Self-Interacting Dark Matter (SIDM) model. We want to see if a change of dark matter species can rescue the hierarchical galaxy formation models.

In Figure 9, we present a comparison of the angular momentum distribution between LCDM-H halos and WDM halos. The mass of the halos are  $6 \times 10^{11} h^{-1} M_{\odot}$  and  $7 \times 10^{10} h^{-1} M_{\odot}$ . From Jing (2001), the streaming effect of WDM is significant at these mass scales. In the top two panels,  $M(< j)/M(j > 0)$  of two LCDM-H halos are presented (triangles and the solid line) together with those of the corresponding WDM halos (open circles and the dotted line). The difference in  $M(< j)/M(j > 0)$  between the two dark matter models is significant, but is not systematic. In the low panels, we show comparisons of the fitting parameter  $\mu$  and the spin parameter  $\lambda$  between LCDM-H and WDM halos. The results clearly show that there is a correlation of the parameters between the two models but the scatter is quite large. The WDM halo may contain a lower (top left) or higher (top right) amount of low  $j$  mass than the corresponding LCDM halo. There is however no indication for any systematic difference in the angular momentum distribution between the two dark matter models. Our results agree well with the recent studies of Knebe et al. (2001) and Bullock et al. (2001b).

The distribution of the angular momentum of halos in SIDM models has similar profiles to those of the LCDM model. Figure 10 presents a comparison of the fitting parameter  $\mu$  and the spin parameter  $\lambda$  between the LCDM ( $\sigma = 0$ ) and SIDM halos. There is a tendency that both  $\mu$  and  $\lambda$  become smaller in the models of stronger interaction (i.e. larger  $\sigma$ ), i.e. the angular momentum is reduced by the dark matter interaction. This indicates that SIDM models may have more difficulties to reproduce the observation data of disk galaxies than the conventional LCDM models.

## 5. Discussion and conclusions

We have studied the angular momentum profile of dark matter halos for a statistical sample drawn from a set of high-resolution cosmological simulations. Two typical CDM models have been considered, and the halos are selected to have at least  $3 \times 10^4$  particles in order to reliably measure the angular momentum profile. In contrast with the recent claims of B2001, we find that the degree of misalignment of the angular momentum within a halo is very high. About 50 percent of halos have more than 10 percent of halo mass in the mass

of negative angular momentum  $j$ . After the mass of negative  $j$  is excluded, the cumulative mass function  $M(< j)$  follows approximately the universal function proposed by B2001 if the virial mass  $M_v$  in the function is replaced by  $M(j > 0)$ , though we still find a significant fraction of halos ( $\sim 50\%$ ) which exhibit systematic deviations from the universal function. Our results, however, are broadly in good agreement with the recent work of van den Bosch et al. (2002).

We have also studied the angular momentum profile of halos in the Warm Dark Matter model and in the Self-Interacting Dark Matter model in order to study how the angular momentum profile is affected by the basic assumption about the dark matter. We have made a detailed comparison between the halos in these scenarios and the corresponding halos in the LCDM model. We find that there is no *systematic* difference in the angular momentum between the halos from the WDM and from the LCDM, though a pair of corresponding WDM and LCDM halos may exhibit quite different angular momentum profiles. We also find that the self-interaction of dark matter in the SIDM models can generally reduce the angular momentum, which makes the spin parameter  $\lambda$  and the shape parameter  $\mu$  smaller. Thus it seems that these dark models do little help to solve the angular momentum problem encountered by the CDM models.

Our results also indicate that it should be cautious to use the universal angular momentum profile of B2001 to predict observational properties for disk galaxies. The angular momentum in different parts of a halo does not orient as coherently as B2001 claimed. The mass of negative angular momentum  $j$  may combine with those mass of small  $j$  to form the bulge component in spiral galaxies (van den Bosch et al. 2002), or the angular momentum profile of the gas in a halo is significantly different from that of the dark matter due to hydro-dynamical processes like heating and explosions (Maller & Dekel 2002). The relation between the disk properties and the angular momentum profile (Eq.1) could be more complicated than previously thought.

We would like to thank van den Bosch for useful discussion. The work is supported in part by the One-Hundred-Talent Program, by NKBRSF(G19990754) and by NSFC(No.10125314).

## REFERENCES

- Avila-Reese, V., Colín, P., Valenzuela, O., D’Onghia, E., & Firmani, C. 2001, ApJ, 559, 516  
 Avila-Reese, V., & Firmani, C. 2000, RevMexAA, 36, 23

- Bardeen, J. M., Bond, J. R., Kaiser, N., & Szalay, A. S., 1986, *ApJ*, 304, 15
- Blumenthal, G. R., Faber, S. M., Flores, R., & Primack, J. R. 1986, *ApJ*, 301, 27
- Bode, P., Ostriker, J. P., & Turok, N., 2001, *ApJ*, 556, 93
- Bryan, G., & Norman, M. 1998, *ApJ*, 495, 80
- Bullock, J. S., Dekel, A., Kolatt, T. S., Kravtsov, A. V., Klypin, A. A., Porciani, C., & Primack, J. R., 2001, *ApJ*, 555, 240 (B2001)
- Bullock, J. S., Kravtsov, A. V., Colín, P., 2001, *astro-ph/0109432*
- Burkert, A., 2000, *ApJ*, 534, L143
- Colombi, S., Dodelson, S., & Widrow, L. M., 1996, *ApJ*, 458, 1
- Dalcanton, J.J., Spergel, D.N., & Summers, F.J., 1997, *ApJ*, 482, 659
- Davé, R., Spergel, D. N., Steinhardt, P. J., & Wandelt, B. D. 2001, *ApJ*, 547, 574
- Fall, S.M., & Efstathiou, G., 1980, *MNRAS*, 193, 189
- Jimenez, R., Heavens, A. F., Hawkins, M. R. S., & Padoan, P. ,1997, *MNRAS*, 292, L5
- Jing, Y.P., 2000, *ApJ*, 535, 30
- Jing, Y.P., 2001, *Mod. Phys. Lett.*, A16, 1795
- Jing, Y.P., Mo, H.J., Börner, G., & Fang, L.Z., 1995, *MNRAS*, 276, 417
- Jing, Y.P., & Suto, Y., 1998, *ApJ*, 494, L5
- Jing, Y.P., & Suto, Y., 2000, *ApJ*, 529, L69
- Klypin, A., Kravtsov, A. V., Valenzuela, O., & Prada, F., 1999, *ApJ*, 522, 82
- Knebe, A., Devriendt, J., Mahmood, A., & Silk, J. 2001, preprint (*astro-ph/0105316*)
- Maller, A. H., & Dekel A., 2002, *astro-ph/0201187*
- Maller, A. H., Dekel A., & Somerville, R., 2002, *MNRAS*, 329, 423
- Moore, B., Ghigna, S., Governato, F., Lake, G., Quinn, T., Stadel, J., & Tozzi, P., 1999, *ApJ*, 524, L19
- Mo, H.J., & Mao, S., 2002, *astro-ph/0112108*
- Mo, H.J., Mao, S., & White, S.D.M., 1998, *MNRAS*, 295, 319 (MMW)
- Navarro, J. F., & Benz, W., 1991, *ApJ*, 380, 320
- Navarro, J. F., Frenk, C. S., & White, S. D. M., 1996, *ApJ*, 462, 563 (NFW)
- Navarro, J.F., & Steinmetz, M., 2000, *ApJ*, 538, 477
- Navarro, J.F., & White, S.D.M., 1994, *MNRAS*, 267, 401

- Schaeffer, R., & Silk, J., 1988, ApJ, 332,1
- Sommer-Larsen, J., & Dolgov, A., 2001, ApJ, 551, 608
- Sommer-Larsen, J., Gelato, S., & Vedel, H., 1999, ApJ, 519, 501
- Spergel, D. N., & Steinhardt, P. J., 2000, Physical Review Letters, 84, 3760
- Steinmetz, M., & Navarro, J. F. 1999, ApJ, 513, 555
- van den Bosch, F. C., 1998, ApJ, 507, 601
- van den Bosch, F. C. 2001, MNRAS, 327, 1334
- van den Bosch, F. C., Abel, T., C. C. R. A., Hernquist, L., & White, S. D. M., 2002, astro-ph/0201095
- van den Bosch, F. C., Burkert, A., & Swaters, R. A. 2001, MNRAS, 326, 1205
- Weil, M. L., Eke, V. R., & Efstathiou, G., 1998, MNRAS, 300, 773
- White, S.D.M., & Reese, M.J., 1978, MNRAS, 183, 341
- Yoshida, N., Springel, V., White, S. D. M., & Tormen, G., 2000, ApJ, 544,L87

Table 1: The probability of two j-distributions drawn from the same parent distribution

CDM Model	Probability
LCDM-H vs LCDM-CM	0.3374
LCDM-H vs LCDM-C	0.8233
LCDM-H vs SCDM-CM	0.1535
LCDM-H vs SCDM-C	0.2261
LCDM-CM vs SCDM-CM	0.8441
LCDM-C vs SCDM-C	0.0026

Table 2: Summary of the simulation models

Model	$L_{box}(h^{-1}\text{Mpc})$	$m_p(h^{-1}M_{\odot})$	$N_v^a$	Number of halos
LCDM-H <sup>b</sup>			$3 \times 10^5$	15
LCDM-C	100(LCDM100)	$5.0 \times 10^9$	$3 \times 10^4$	426
	50(LCDM50)			
LCDM-CM	100(LCDM100)	$5.0 \times 10^9$	$10^5$	10
	50(LCDM50)			
SCDM-C	100(SCDM100)	$1.7 \times 10^{10}$	$3 \times 10^4$	522
	50(SCDM50)			
SCDM-CM	100(SCDM100)	$1.7 \times 10^{10}$	$10^5$	27
	50(SCDM50)			

<sup>a</sup>The minimum number of particles per halo

<sup>b</sup>The boxsize and mass of the particles are varied

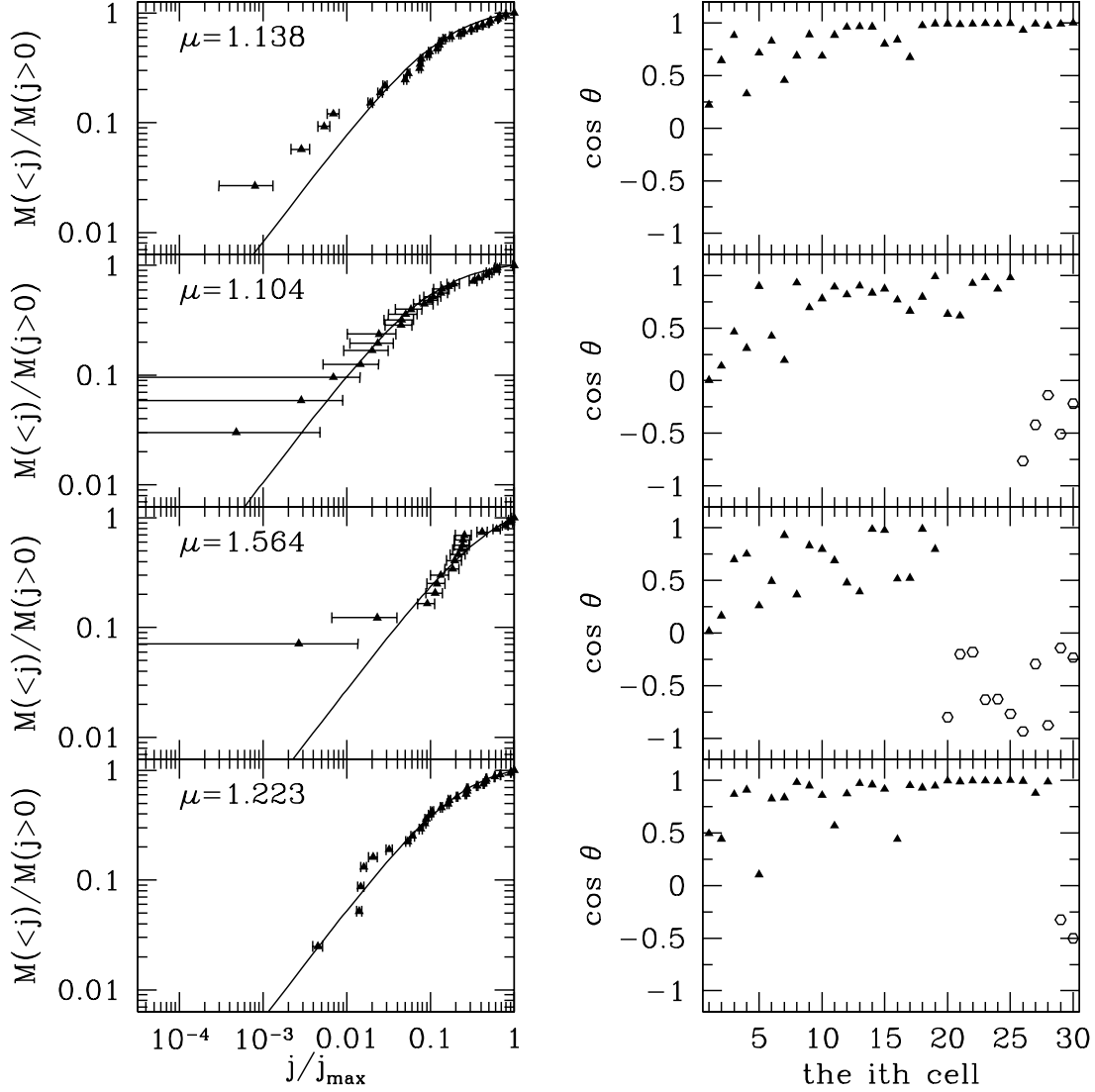


Fig. 1.— *Left panel* – the mass distribution of specific angular momentum of four halos in the LCDM model. *Right panel* – the  $\cos \theta$  of the cells in the corresponding halos. Solid and open symbols are used for positive and negative values of  $\cos \theta$  respectively.

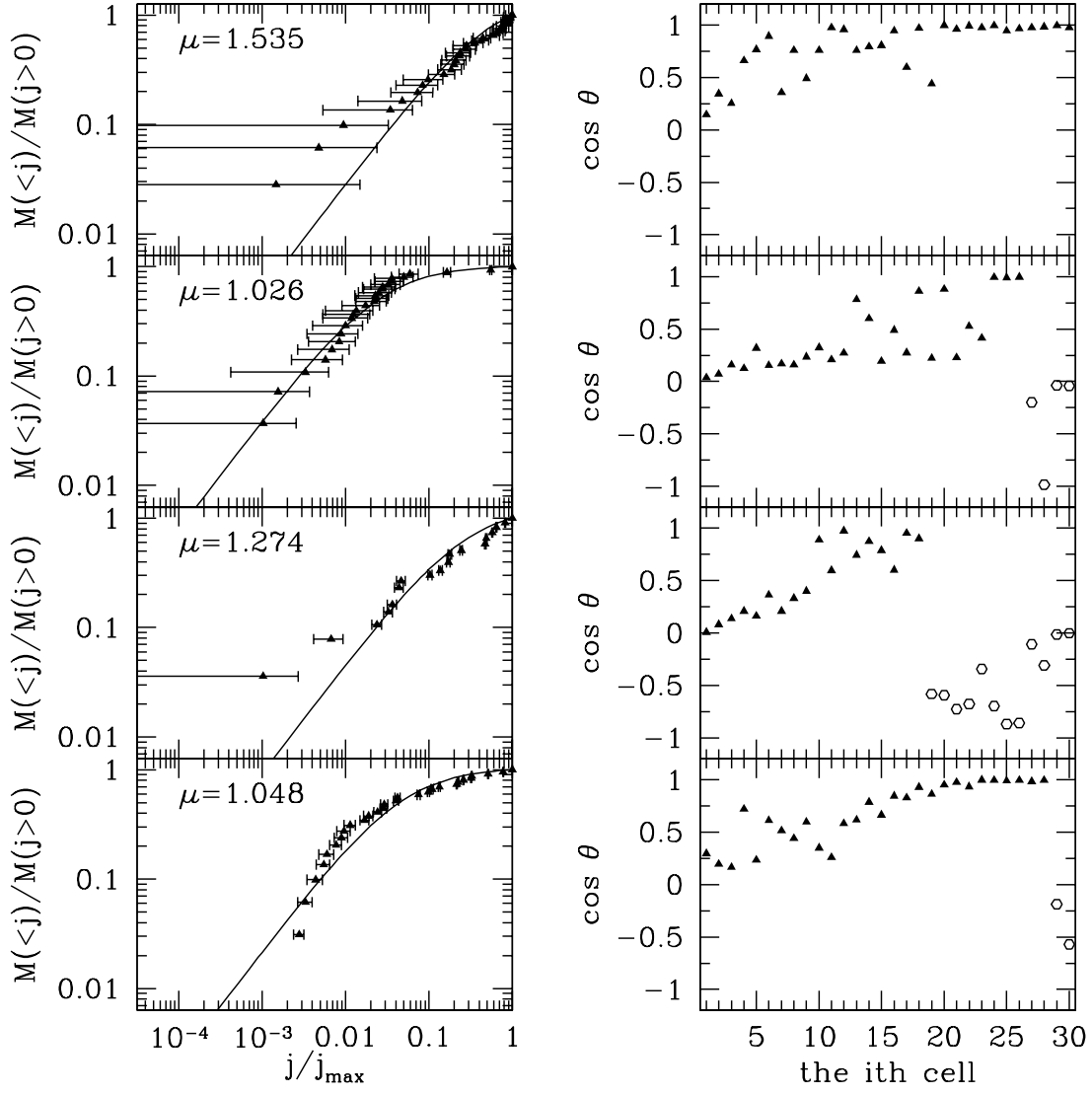


Fig. 2.— The same as Fig. 1, but for four halos in the SCDM model.

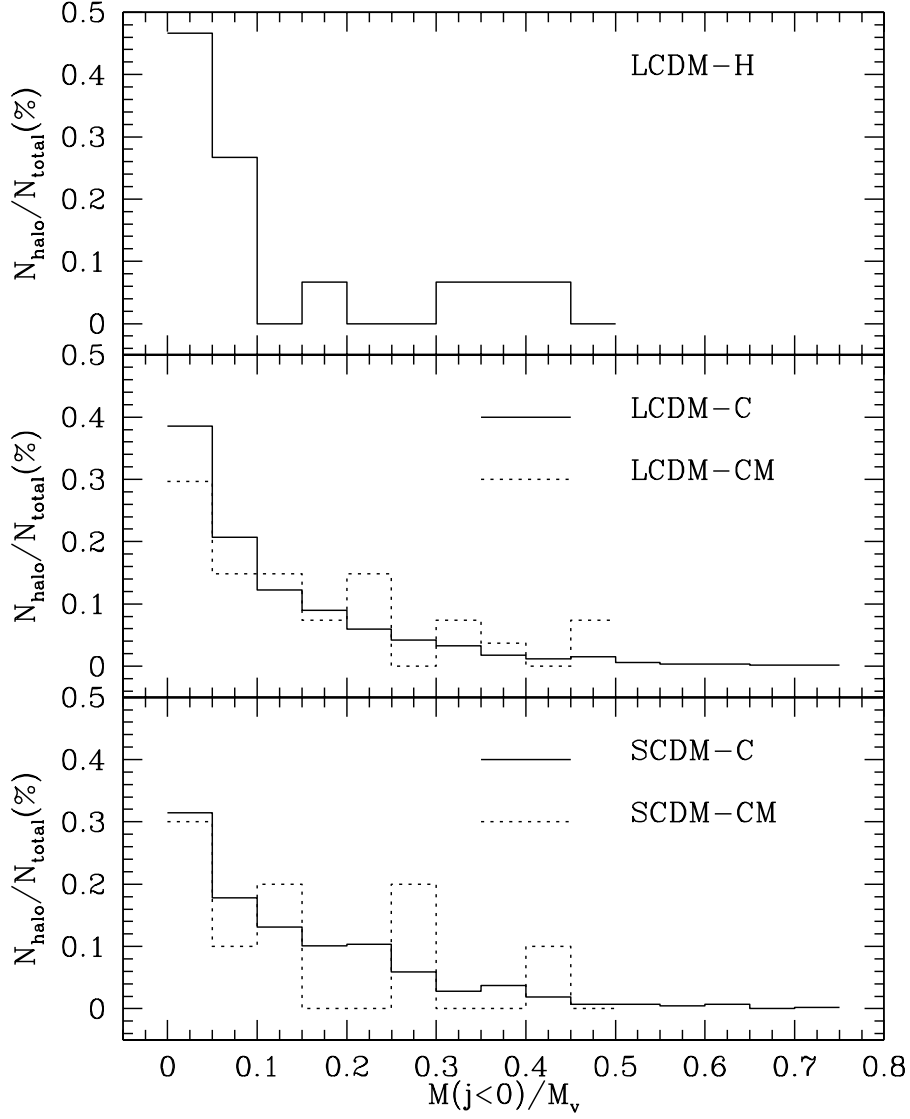


Fig. 3.— The percentage of halos having mass  $M(j < 0)$  contained in negative  $j$  cells. LCDM-H halos are shown in the top panel. In the middle panel, the solid histogram is for the LCDM-C halos and the dot one for the LCDM-CM halos. In the bottom panel, the solid and dotted histograms are for SCDM-C and SCDM-CM respectively



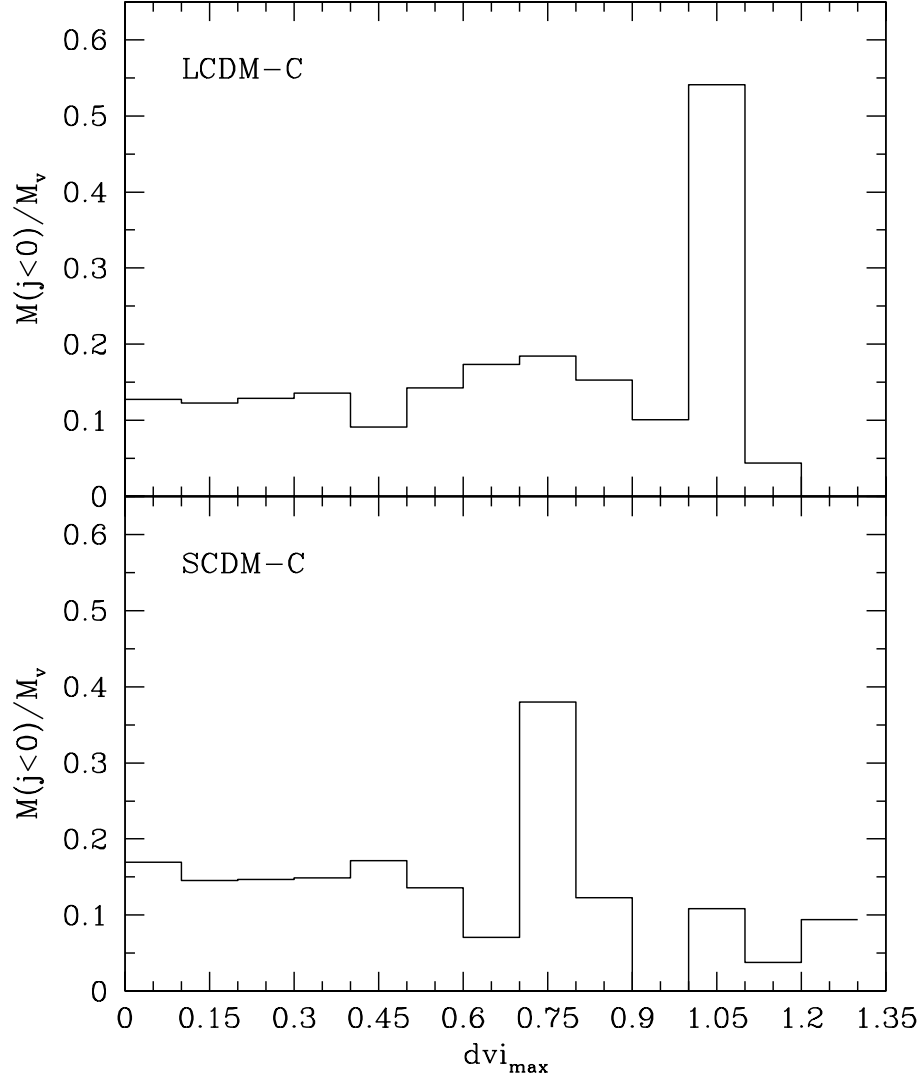


Fig. 4.— The total mass of negative  $j$  cells vs the substructure indicator  $dvi_{\max}$  for both LCDM and SCDM models.

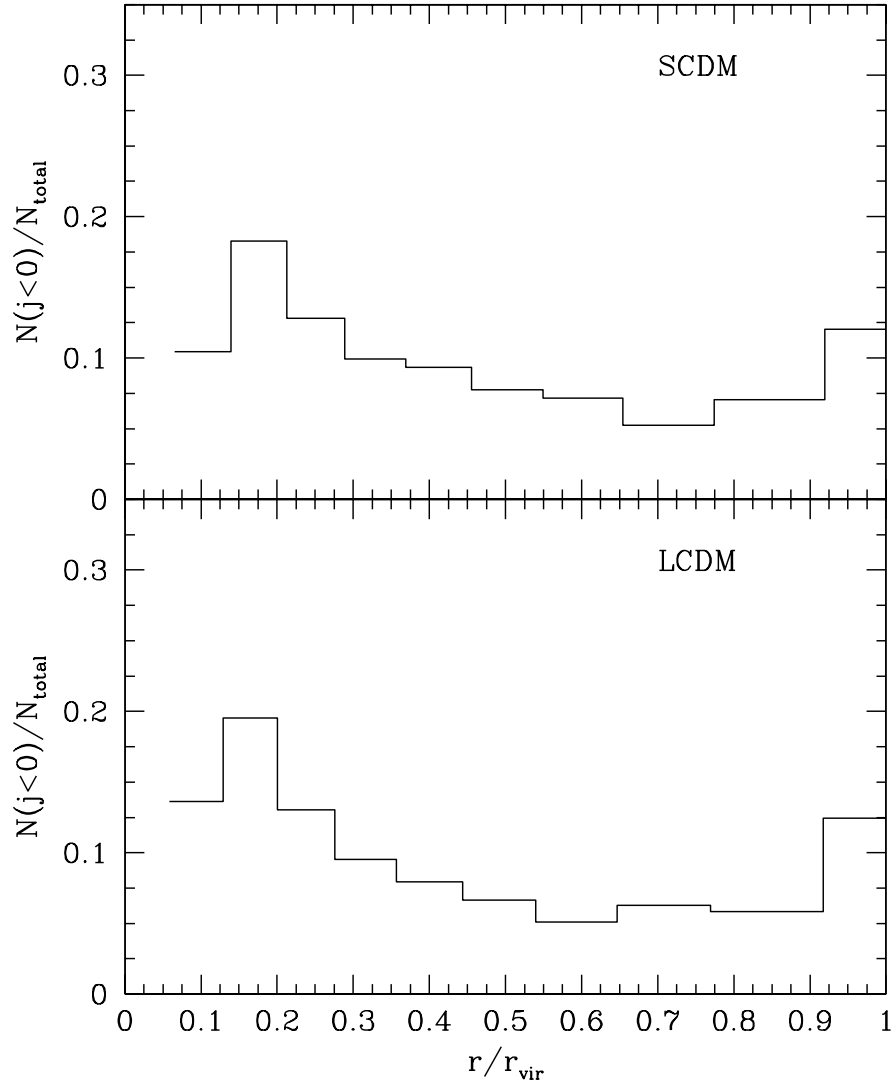


Fig. 5.— The percentage of negative  $j$  cells at radius  $r$ .

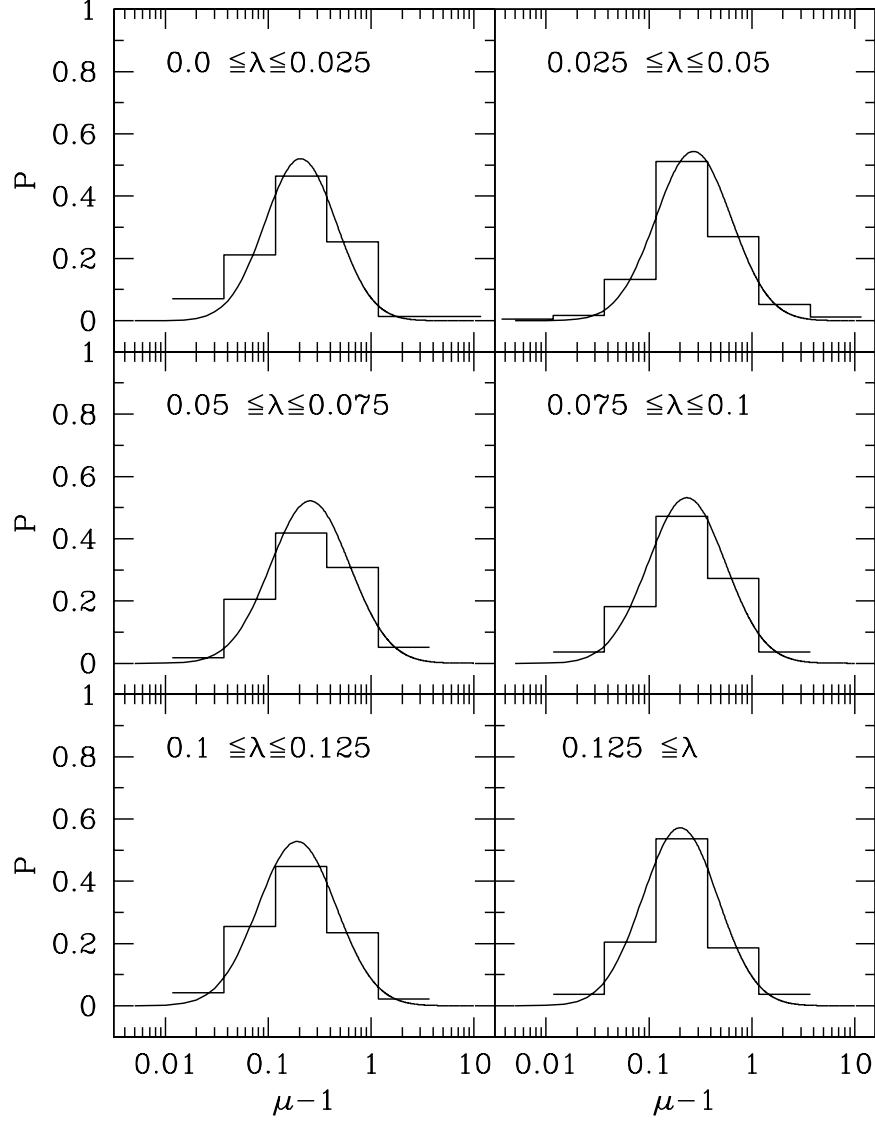


Fig. 6.— The  $\mu$  distribution of halos for LCDM model(histogram). Halos were divided into six groups according to their  $\lambda$  values. The solid curves in each panel are the log-normal distributions of  $\mu - 1$  with the means and the standard deviations shown in Fig.8

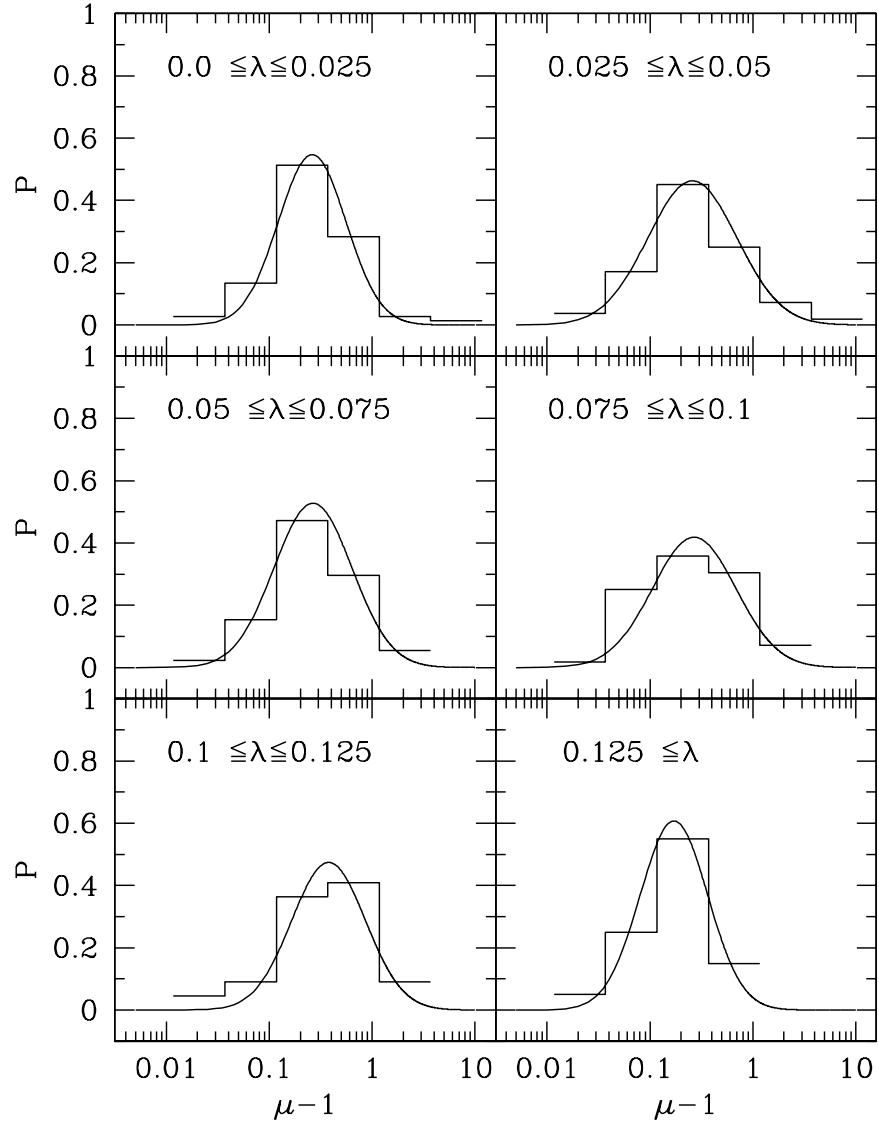


Fig. 7.— The same as Fig.6 but for the SCDM model.

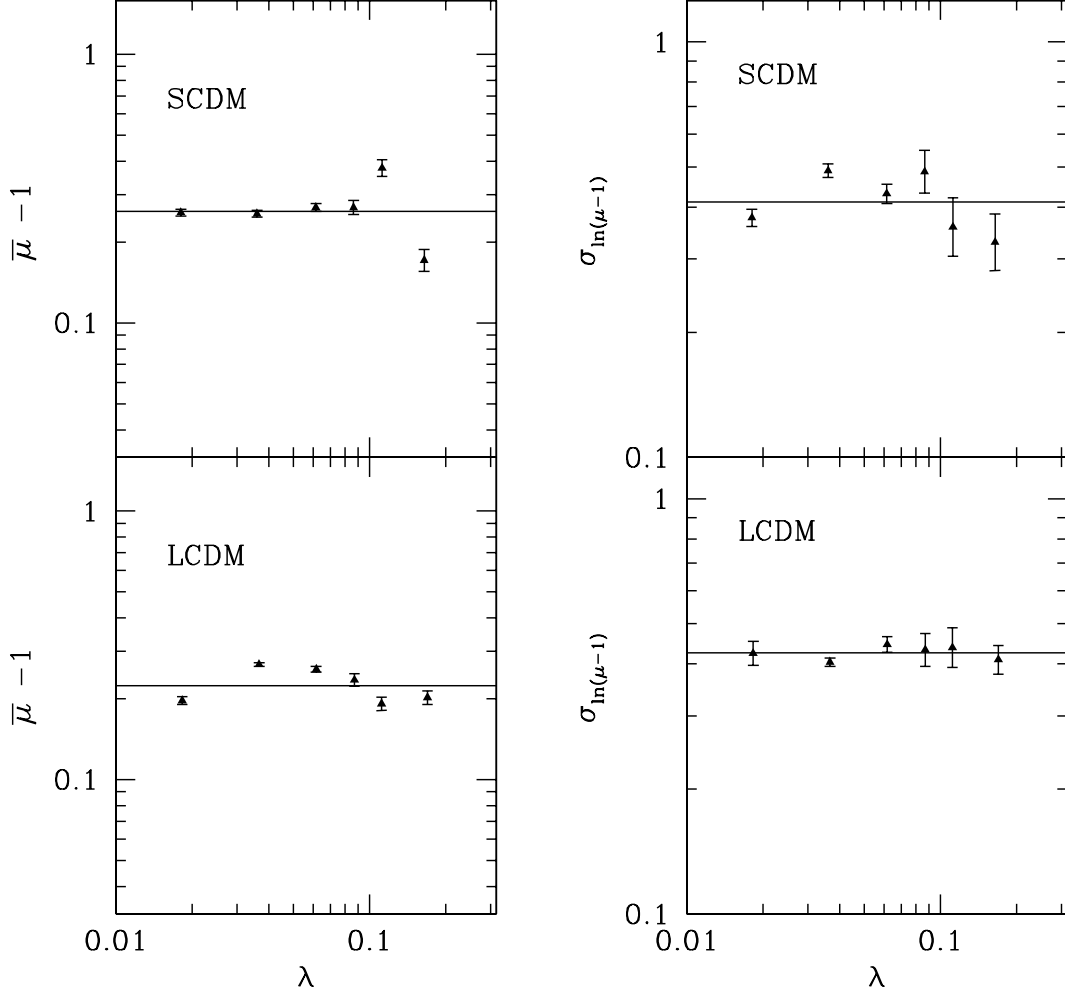


Fig. 8.— The means and standard deviations of the log-normal distribution of  $\mu - 1$  for both LCDM and SCDM model as a function of  $\lambda$ . The solid lines are the average values.

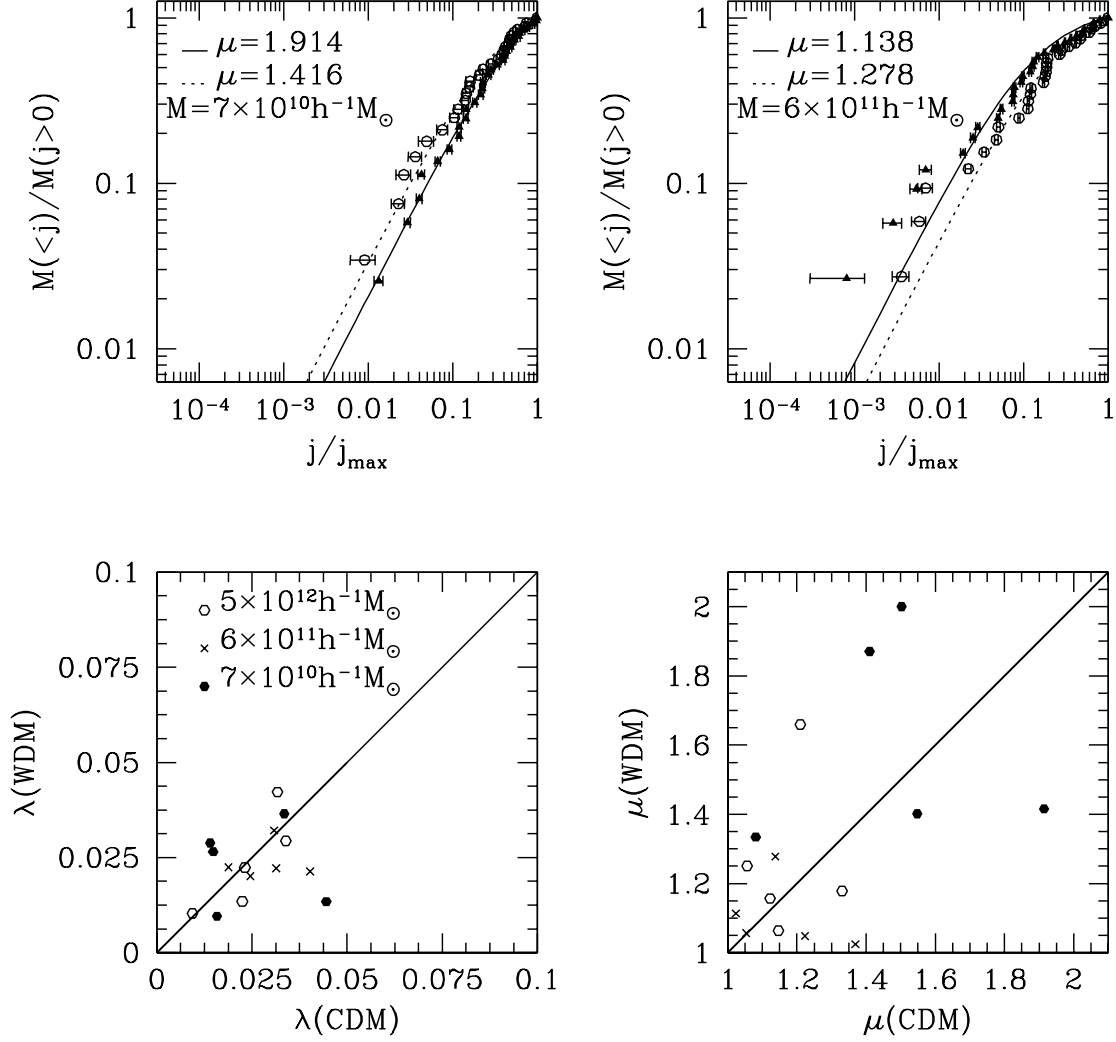


Fig. 9.— *Upper panels* – The cumulative mass  $M(<j)$  as a function of the specific angular momentum  $j$  for two pairs of LCDM and WDM halos. Open circles and dotted lines are for the WDM halos, and filled triangles and solid lines for LCDM halos. *Lower panels* – The spin parameter  $\lambda$  and shape parameter  $\mu$  of the WDM halos vs. those of the LCDM halos.

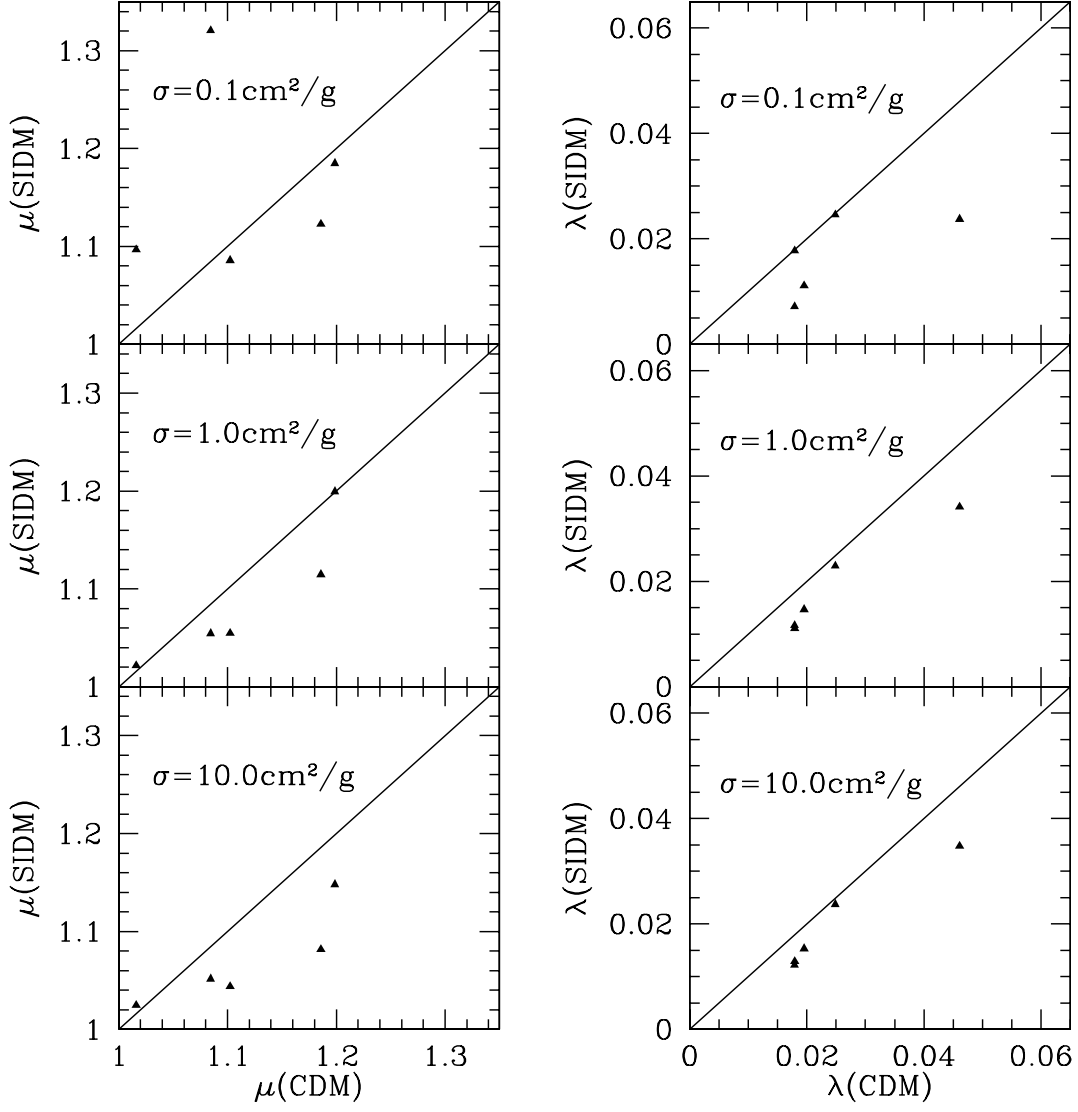


Fig. 10.— The spin parameter  $\lambda$  and shape parameter  $\mu$  of the SIDM halos vs. those of the LCDM halos.